Science Journal of Chemistry
2023; 11(2): 56-63
http://www.sciencepublishinggroup.com/j/sjc
doi: 10.11648/j.sjc.20231102.13
ISSN: 2330-0981 (Print); ISSN: 2330-099X (Online)

Spectroscopic Studies and X-ray Structural of Dinuclear Lanthanide (III) Complexes Derived from N'-(2-hydroxy-3-methoxybenzylidene) Nicotinohydrazide

Fatou Barr[1], Papa Samba Camara[1], Amadou Guèye[2], Sofia Zazouli[3], Nathalie Gruber[4], Farba Bouyagui Tamboura[1], Moussa Dieng[1], Mohamed Gaye[2, *]

[1]Department of Chemistry, University Alioune Diop, Bambey, Senegal

[2]Department of Chemistry, University Cheikh Anta Diop, Dakar, Senegal

[3]Faculty of Sciences and Technologies, Sultan Moulay Slimane University, Beni-Mellal, Morocco

[4]CNRS UMR 7140, University of Strasbourg, Strasbourg, France

Email address:

mohamedl.gaye@ucad.edu.sn (Mohamed Gaye)

[*]Corresponding author

To cite this article:

Fatou Barr, Papa Samba Camara, Amadou Guèye, Sofia Zazouli, Nathalie Gruber, Farba Bouyagui Tamboura, Moussa Dieng, Mohamed Gaye. Spectroscopic Studies and X-ray Structural of Dinuclear Lanthanide (III) Complexes Derived from N'-(2-hydroxy-3-methoxybenzylidene) Nicotinohydrazide. *Science Journal of Chemistry*. Vol. 11, No. 2, 2023, pp. 56-63. doi: 10.11648/j.sjc.20231102.13

Received: April 2, 2023; **Accepted**: April 17, 2023; **Published**: April 27, 2023

Abstract: Two Schiff bases (H_2L), derived from o-vanillin and nicotinic hydrazide, and its complexes with some lanthanides (Y, Ce, Yb, Pr, Gd and Tb) have been synthesized. These compounds have been characterized by means of elemental analysis, UV–Vis spectroscopy, FTIR spectroscopy, ^1H and ^{13}C NMR (for H_2L), molar conductance and room temperature magnetic measurements. The compounds are found isostructural and are formulated as $\{[(Z)(\eta^2\text{-}OOCH_3)Ln](\mu\text{-}L)_2[Ln(\eta^2\text{-}OOCH_3)(Z)]\}$ ($Z = H_2O$ for Ln = Y, Ce, Pr, Gd or Tb and $Z = OS(CH_3)_2$ for Ln =Yb). The two ligand molecules act in their dideprotonated forms through one azomethine nitrogen atom, one phenoxo oxygen atom and one iminolate oxygen atom. The two Ln (III) ions are bridged by two phenoxo oxygen atoms, forming a dinuclear complex. Single crystal X-ray analysis of the ytterbium complex has revealed the nature of the structure $\{[(OS(CH_3)_2)(\eta^2\text{-}OOCH_3)Yb](\mu\text{-}L)_2[Yb(\eta^2\text{-}OOCH_3)(OS(CH_3)_2)]\}$ (3). The complex crystallizes in the monoclinic space group C2/c with cell parameters of a = 13.0391(6) Å, b = 15.1199(6) Å, c = 20.7239(7) Å, β = 105.671(2)°, V = 3933.8(3) Å^3, Z = 4, R_1 = 0.025, wR_2 = 0.65. The ytterbium atoms are eight-coordinated, and their coordination polyhedron are best described as a square antiprismatic geometry. The aromatic rings of the ligand molecule are twisted with dihedral angle of 29.23 (1)° between their mean planes.

Keywords: Hydrazide, Lanthanide, FTIR, NMR, Crystal, X-ray Diffraction

1. Introduction

Macrocyclic ligands are widely used in the coordination chemistry of lanthanide ions to yield complexes with exceptional physicochemical properties [1–4]. These organic ligands resulting from condensation reactions between ketoprecursors and amine derivatives such as hydrazones present inners which can encapsulated metal cations [5]. Several cyclic and acyclic compounds [6–8] have been synthetized using original methods in synthetic organic chemistry [9]. These organic ligands [10] have, in some cases, very interesting properties such as antifungals and antibacterial [11]. The interest in the chemistry of lanthanide ions has increased very rapidly in a few decades because of their multiple modes of coordination [12]. Particular attention has been paid to these metals due to their low toxicity, their potential to be used as biological diagnostic agents and their paramagnetic [13–15] and luminescent [16, 17] properties [18, 19]. Several applications of lanthanide complexes continue to arouse the curiosity of the scientific community [20]. They are used as catalysts [21, 22] in transesterification [23, 24], and radiopharmaceuticals [25, 26]. Some Eu (III) and Nd (III)

complexes have been reported to have a laser property [27]. We have reported in the past N_5O_2 ligands [28, 29] and N_4O_3 ligands [30] that possess large cavities that can encapsulate one or more lanthanide ions. We have been interested in several years in acyclic ligands of the O_2NO type to build homobinuclear complexes of lanthanides (III). In this work we present the reaction between lanthanide (III) acetates and N'-(2-hydroxy-3-methoxybenzylidene)nicotinohydrazide (H_2L). The resulting complexes are characterized using spectroscopic techniques and by X-ray diffraction.

2. Experimental Section

2.1. Starting Materials and Instrumentations

o-Vanillin and nicotinic hydrazide were purchased from Sigma-Aldrich and used as received without further purification. Solvents were of analytical reagent grade and were used directly without further purification. Elemental analyses of C, H and N were recorded on a VxRio EL Instrument. Infrared spectra were obtained on a FTIR Spectrum Two of Perkin Elmer spectrometer in the 4000-400 cm^{-1} region. The UV-Visible spectra were recorded on a Perkin Elmer Lambda UV-Vis spectrophotometer. The molar conductance of 1×10^{-3} M in DMF solutions of the metal complexes was measured at 25°C using a WTW LF-330 conductivity meter with a WTW conductivity cell. Room temperature magnetic susceptibilities of the powdered samples were measured using a Johnson Mattey scientific magnetic susceptibility balance (Calibrant: $Hg[Co(SCN)_4]$).

2.2. Synthesis of the Ligand N'-(2-hydroxy-3-methoxybenzylidene) nicotinohydrazide (H_2L)

To a solution of o-vanillin (3.0 g, 19.7 mmol) in 20 mL of ethanol was added dropwise a solution of nicotinic hydrazide (2.702 g, 19.7 mmol) in 20 mL of ethanol. The mixture was stirred under reflux for 2 hours. On cooling, the yellow precipitate was isolated by filtration and successively washed with 2 x 10 mL of ethanol and dried in air. Yield: 81.2%. M.P. 95°C. Analytical for $C_{14}H_{13}N_3O_3$: Calc (found) %C, 61.99 (62.03); %H, 4.83 (4.80); %N, 15.49 (15.44). FTIR (ν, cm^{-1}): 3333 (NH); 3200 (OH); 1654 (C=O); 1603 (C=N); 1570; 1474; 1420 C_{Ar}=C_{Ar}; 1300 (C-O_{phenol}); 1242 (C-O_{ether}); 1075 (N-N); 890, 833, 777, 721 and 706 (C—H_{Ar}). UV-vis (DMF, λ (nm)): 273; 337; 372. ^{1}H NMR (dmso-d_6, δ (ppm)): 12.21 (S, OH, 1H); 10.78 (S, NH, 1H); 9.09 (s, HC=N, 1H); [6.80-8.29] (m, H_{arom}, 7H); 3.82 (s, —OCH_3, 3H). ^{13}C NMR (dmso-d_6. δ (ppm)): 161.33 (C=O); 152.38 (C=N); 148.56 (C—O_{phenol}); 148.24 (C—O_{ether}); [147.88 (C_{Ar}), 147.04 (C_{Ar}), 135.40 (C_{Ar}), 128.57 (C_{Ar}), 120.60 (C_{Ar}), 120.39 (C_{Ar}), 119.03 (C_{Ar}), 113.75 (C_{Ar}); 55.74 (—OCH_3).

2.3. General Synthesis of {[(H_2O)(η^2-$OOCH_3$)Ln](μ-L)$_2$[Ln(η^2-$OOCH_3$)(H_2O]} Complexes

In a flask containing 10 mL of ethanol, introduce (0.1 g, 0.369 mmol) of the H_2L organic ligand. $Ln(OOCCH_3)_3.xH_2O$ (Ln = Y, Ce, Gd, Pr, Tb, Yb), (0.369 mmol) previously dissolved in 10 mL of ethanol was added to the flask. The mixture obtained is stirred for one hour. The precipitate which appears was subsequently heated under reflux for one hour. After cooling, the solid was collected by filtration, washed with ethanol and diethyl ether and dried in air. Recrystallization in DMSO afforded crystals after two weeks of slow evaporation. For the Yb (III) complex, crystals suitable for X-ray analysis were isolated for the complex.

{[(H_2O)(η^2-$OOCH_3$)Y](μ-L)$_2$[Y(η^2-$OOCH_3$)(H_2O]} (1). Yield: 32.99 (%). color: Yellow. M.P. 230°C. Analytical for $C_{32}H_{32}Y_2N_6O_{12}$: Calc (found) %C, 44.15 (44.12); %H, 3.71 (3.78); %N, 9.65 (9.67). UV-vis (DMF, λ (nm)): 240, 335, 385, 405, 478. Diamagnetic. Λ (Ω^{-1} cm^2 mol^{-1}, DMF): 06. ν (cm^{-1}): 1599, 1528, 1455, 1374, 1218, 1087.

{[(H_2O)(η^2-$OOCH_3$)Ce](μ-L)$_2$[Ce(η^2-$OOCH_3$)(H_2O]} (2). Yield: 33.92 (%). Color: Green. M.P. 240°C. Analytical for $C_{32}H_{32}Ce_2N_6O_{12}$: Calc (found) %C, 39.51 (39.53); %H, 3.32 (3.36); %N, 8.64 (8.61). UV-vis (DMF, λ (nm)): 242, 325, 388, 400, 478. μ_{eff} = 2.47 μ_B. Λ ($\Omega^{-1}cm^2$ mol^{-1}, DMF): 08. ν (cm^{-1}): 1603, 1552, 1440, 1360, 1214, 1070.

{[($OS(CH_3)_2$)(η^2-$OOCH_3$)Yb](μ-L)$_2$[Yb(η^2-$OOCH_3$)($OS(CH_3)_2$)]} (3). Yield: 33.77 (%). Color: Yellow. M.P. 240°C. Analytical for $C_{36}H_{40}Yb_2N_6O_{12}S_2$: Calc (found) %C, 37.31 (37.29); %H, 3.48 (3.52); %N, 7.25 (7.28); %S 5.53 (5.51). UV-vis (DMF, λ (nm)): 257; 283; 303; 360; 376; 402. μ_{eff} = 3.81μ_B. Λ ($\Omega^{-1}cm^2$ mol^{-1}, DMF): 07. ν (cm^{-1}): 1602, 1586, 1457, 1377, 1219, 1080.

{[(H_2O)(η^2-$OOCH_3$)Pr](μ-L)$_2$[Pr(η^2-$OOCH_3$)(H_2O]} (4). Yield: 42.00 (%). Color: Green. M.P. 240°C. Analytical for $C_{32}H_{32}Pr_2N_6O_{12}$: Calc (found) %C, 39.44 (39.40); %H, 3.31 (3.29); %N, 8.62 (8. 59. UV-vis (DMF, λ (nm)): 240, 328, 382, 402, 476. μ_{eff} = 3.21μ_B. Λ ($\Omega^{-1}cm^2$ mol^{-1}, DMF): 07. ν (cm^{-1}): 1618, 1555, 1444, 1364, 1214, 1084.

{[(H_2O)(η^2-$OOCH_3$)Gd](μ-L)$_2$[Gd(η^2-$OOCH_3$)(H_2O]} (5). Yield: 38.86 (%). Color: Yellow. M.P. 235°C. Analytical for $C_{32}H_{32}Gd_2N_6O_{12}$: Calc (found) %C, 38.16 (38.12); %H, 3.20 (3.19); %N, 8.34 (8.31). UV-vis (DMF, λ (nm)): 242, 332, 382, 402, 477. μ_{eff} = 7.49 μ_B. Λ ($\Omega^{-1}cm^2$ mol^{-1}, DMF): 02. ν (cm^{-1}): 1608, 1560, 1446, 1365, 1214, 1071.

{[(H_2O)(η^2-$OOCH_3$)Tb](μ-L)$_2$[Tb(η^2-$OOCH_3$)(H_2O]} (6). Yield: 40.50 (%). Color: Yellow. M.P. 235°C. Analytical for $C_{32}H_{32}Tb_2N_6O_{12}$: Calc (found) %C, 38.04 (38.00); %H, 3.19 (3.15); %N, 8.32 (8.29). UV-vis (DMF, λ (nm)): 242, 329, 385, 403, 477. μ_{eff} = 4.38 μ_B. Λ (Ω^{-1} cm^2 mol^{-1}, DMF): 08. IR ν (cm^{-1}): 1610, 1538, 1450, 1369, 1217, 1074.

2.4. Crystal Structure Determination

Crystals suitable for single-crystal X-ray diffraction, of the reported compound (1), were grown by slow evaporation of MeOH solution of the complex. Details of the crystal structure solution and refinement are given in Table 1. Diffraction data were collected using a Bruker Apex II with graphite monochromatized MoKα radiation (λ = 0.71073 Å). All data were corrected for Lorentz and polarization effects. Complex scattering factors were taken from the program package

SHELXTL [31]. The structures were solved by direct methods which revealed the position of all non-hydrogen atoms. All the structures were refined on F^2 by a full-matrix least-squares procedure using anisotropic displacement parameters for all non-hydrogen atoms [32]. H atoms (NH, OH, CH and CH_3 groups) were geometrically optimized and refined as riding model by AFIX instructions. Molecular graphics were generated using ORTEP [33].

3. Results and Discussion

3.1. General Study

The infrared spectrum of the ligand (Table 1) presents towards the high frequencies a fine band pointed at 3543 cm^{-1}. This band is attributed to the vibration of the N—H bond. The other bands pointed at 3200 and 3068 cm^{-1} are respectively attributed to the valence vibrations of the hydroxyl group (OH) and the C—H (aromatic) bonds. The valence vibration of the carbonyl (C=O) is pointed at 1654 cm^{-1} and that of the imine function at 1603 cm^{-1}. Between 1570 and 1420 cm^{-1} we identify the vibrations of the C=N and C=C bonds of the two pyridine and aromatic nuclei. A strong band at 1366 cm^{-1} is attributed to the vibration of the C—N bond. The presence of this band and that of $\nu_{C=O}$ indicates that the ligand is in its amide form. The bands pointed at 1300 cm^{-1} and 1242 cm^{-1} are respectively attributed to the vibrations of the phenolic and/or ether C—O bond. The vibration of the N—N bond is located at 1075 cm^{-1}. Deformation vibrations of aromatic C-H bonds appear in the range 890—706 cm^{-1}. ^1H proton, ^{13}C carbon NMR were recorded using dimethylsulfoxide solutions. The ^1H NMR spectrum reveals a singlet signal at 12.21 ppm which represents one proton attributed to the hydroxyl proton OH. Three singlets pointed at 10.78; 9.09 and 8.29 ppm representing one proton each are attributed respectively to NH, HC=N and H_{Ar}. The signal due to the remaining six protons of the two aromatic rings appear as multiplets in the ranges (6.82 - 7.57) and (8.66 - 8.78) ppm. The singlet signal located at 3.82 ppm is due to the three protons of the methoxy group (—OCH_3). The ^{13}C NMR spectrum reveals a signal at 161.33 ppm attributed to the carbon atom of the carbonyl function (C=O). The signal due to the azomethine carbon atom is pointed at 152.38 ppm. The aromatic carbon atoms, present signal in the range 148.52—113.75 ppm. The signal pointed at 55.74 is attributed to the carbon atom of the methoxy group (—OCH_3). The DEPT 135 NMR spectrum indicates the absence of the signal due to the totally substituted quaternary carbon atoms as expected. The mass spectrum of H_2L shows a basic peak located at m/z = 272.10 corresponding to the molar mass of the molecular ion (M+1) of the product. This result makes it possible to determine the molecular formula as $C_{14}H_{13}N_3O_3$ for the ligand.

Upon coordination with lanthanide ions, the band pointed in the FTIR spectrum of the H_2L ligand at 1654 cm^{-1} ($\nu_{C=O}$) disappears and new bands attributed to the formation of a new C=N function appears in the range [1618—1599 cm^{-1}]. This related azomethine nitrogen atom remains uncoordinated. The bands at 1603, 1242 and 1160 cm^{-1}, attributed respectively, to the vibrations $\nu_{C=N}$, $\nu_{C—Ophenol}$, and $\nu_{C—Oether}$ in the ligand were shifted on the FTIR spectra of lanthanide complexes (Table 1) to low frequencies and appears in the ranges [1560—1528 cm^{-1} for $\nu_{C=N}$], [1218—1214 cm^{-1} for $\nu_{C—Ophenol}$] and [1087—1070 cm^{-1} for $\nu_{C—Oether}$] [34]. These facts indicate the involvement of the oxygen atoms of the hydrazonic moiety in its iminolate forms, the phenol and the methoxy groups as well as the azomethine nitrogen atom in the coordination to the relative lanthanide ion. In whole spectra, a broad band is pointed in the region [3450—3200 cm^{-1}] and attributed to the sum of $\nu_{N—H}$ of the hydrazone moiety and $\nu_{O—H}$ of the coordinated water molecule vibrations [35–37]. Additionally, a deformation band $\delta_{O—H}$ is observed in the range [850—830 cm^{-1}]. The two vibration bands ν_{as} and ν_s due to the acetate group are identified on the spectra of the complexes respectively in the ranges [1457—1440 cm^{-1}] and [1377—1360 cm^{-1}]. The magnitude $\Delta\nu = \nu_{as} - \nu_s$ value of *ca.* 80 cm^{-1} is indicative of a bidentate chelating group [12].

The molar conductivity measurements (Table 1) of the complexes recorded from a freshly prepared millimolar solution of DMF and after one week of storage give very low values between 2 and 8 $\Omega^{-1}.cm^2.mol^{-1}$ which indicate a neutral electrolyte in nature according to Geary [38]. The complexes are stable in solution. Electronic spectra of the complexes, recorded in DMF, show absorption bands in the ranges [242—335 nm] and [385—405 nm] nm attributed to the $\pi\rightarrow\pi^*$ and $n\rightarrow\pi^*$ transitions within the ligand. The new band observed, in each spectrum, at *ca*. 477 nm is assigned to the transfer band of the ligand to the Ln^{3+} ions.

All the complexes are diamagnetic except the yttrium complex (1) which is diamagnetic in nature. However, the values of magnetic moments (Table 1) found remain low compared to those of free ions, calculated by Van Vleck [39]. This difference suggests the existence of magnetic interactions between two metal centers of an antiferromagnetic nature according to studies by Ishikawa et al. [38]. These interactions are mediated by phenolate bridges as indicated by Xiong et al. [39]. This fact leads to the conclusion of dinuclear complexes.

Table 1. *The main infrared data, UV-visible and magnetic data of the complexes.*

	$\nu_{C=N}$ (free)	$\nu_{C=N}$(cood)	$\nu_{C—O}$	$\nu_{C—N}$	$OOCCH_3$			DMF, λ (nm)	Λ (Ω^{-1} cm^2 mol^{-1})	μ_{eff} (μ_B)
					ν_{as}	ν_s	Δν			
H_2L	1654	1603	1242	1160	-	-	-	242, 306, 335, 400	-	-
1	1599	1528	1218	1087	1455	1374	81	240, 335, 385, 405, 478	6	-
2	1603	1552	1214	1070	1440	1360	80	242, 325, 388, 400, 478	8	2.47
3	1602	1586	1219	1080	1457	1377	80	240, 331, 382, 405, 484	7	3.81

	$\nu_{C=N}$ (free)	$\nu_{C=N}$(cood)	ν_{C-O}	ν_{C-N}	OOCCH$_3$			DMF, λ (nm)	Λ (Ω^{-1} cm^2 mol^{-1})	μ_{eff} (μ_B)
					ν_{as}	ν_s	Δν			
4	1618	1555	1214	1084	1444	1364	80	240, 328, 382, 402, 476	7	3.21
5	1608	1560	1214	1071	1446	1365	81	242, 332, 382, 402, 477	2	7.49
6	1610	1538	1217	1074	1450	1369	81	242, 329, 385, 403, 477	8	4.38

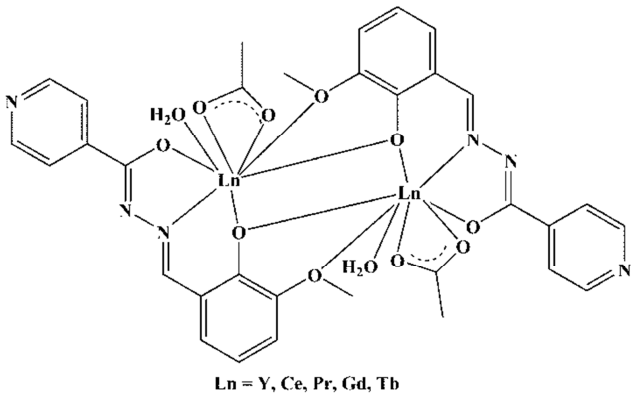

Figure 1. *Proposed structure.*

Based on spectroscopic, magnetic, conductimetric, as well as microanalysis analyzes, the complexes are isostructural. The ligand acts in tetradentate fashion through one azomethine nitrogen atom, one hydrazonic oxygen atom, one bridged phenolate oxygen atom, while the methoxy oxygen atom being coordinated to the second lanthanide ion. One monocoordinated solvent molecule (H_2O or DMSO) and one acetate anion acting in bidentate chelating fashion are present in the coordination sphere of each lanthanide ion, resulting in an eight coordinated lanthanide ion. The proposed structure is illustrated in Figure 1.

3.2. Crystallographic Study of {[(OS(CH$_3$)$_2$)(η^2-OOCH$_3$)Yb](μ-L)$_2$[Yb(η^2-OOCH$_3$)(OS(CH$_3$)$_2$)]} (3)

The complex crystallizes in the monoclinic space group C2/c. Labelled plot of the dinuclear ytterbium complex 3 is shown in Figure 2, the coordination polyhedron of the Yb^{III} ion is shown in Figure 3. Selected interatomic distances and angles are listed in Table 3. The structure of complex 3 consists of {[(OS(CH$_3$)$_2$)(η^2-OOCH$_3$)Yb](μ-L)$_2$[Yb(η^2-OOCH$_3$)(OS(CH$_3$)$_2$)]} discrete entities. The coordination of the ligand to the ytterbium complex occurs via the phenolate oxygen, the hydrazonic oxygen atom, the azomethine nitrogen atom and the methoxy oxygen atom yielding a dinuclear entity. The coordination of the ligand to the Yb^{III} results in the formation of one five and six membered rings YbOCNN and one YbOCCCN with bite angle values of 66.96 (2)° and 77.01 (9)°, respectively. For each Yb of the dinuclear unit, two oxygen atoms from a bidentate acetate groups and one oxygen atom from a dimethylsulfoxide molecule complete the coordination sphere yielding an eight-coordinated geometry.

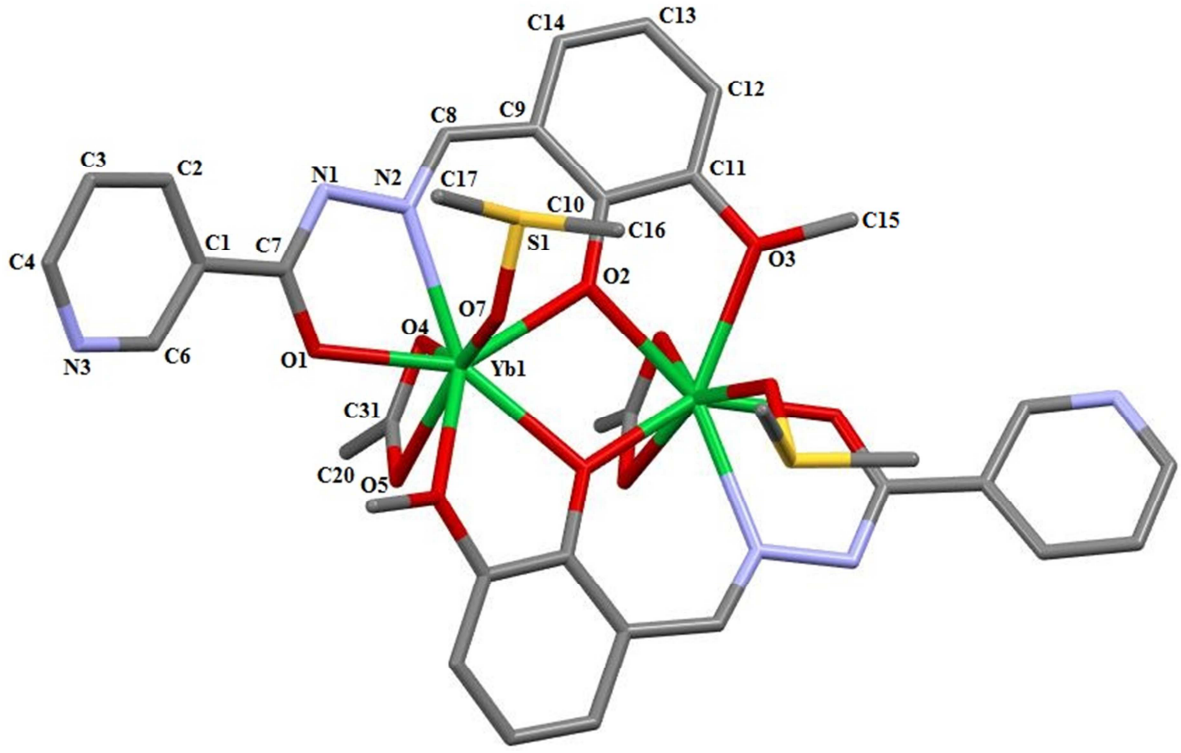

Figure 2. *The ORTEP diagram complex 3, with 50% thermal ellipsoid probability.*

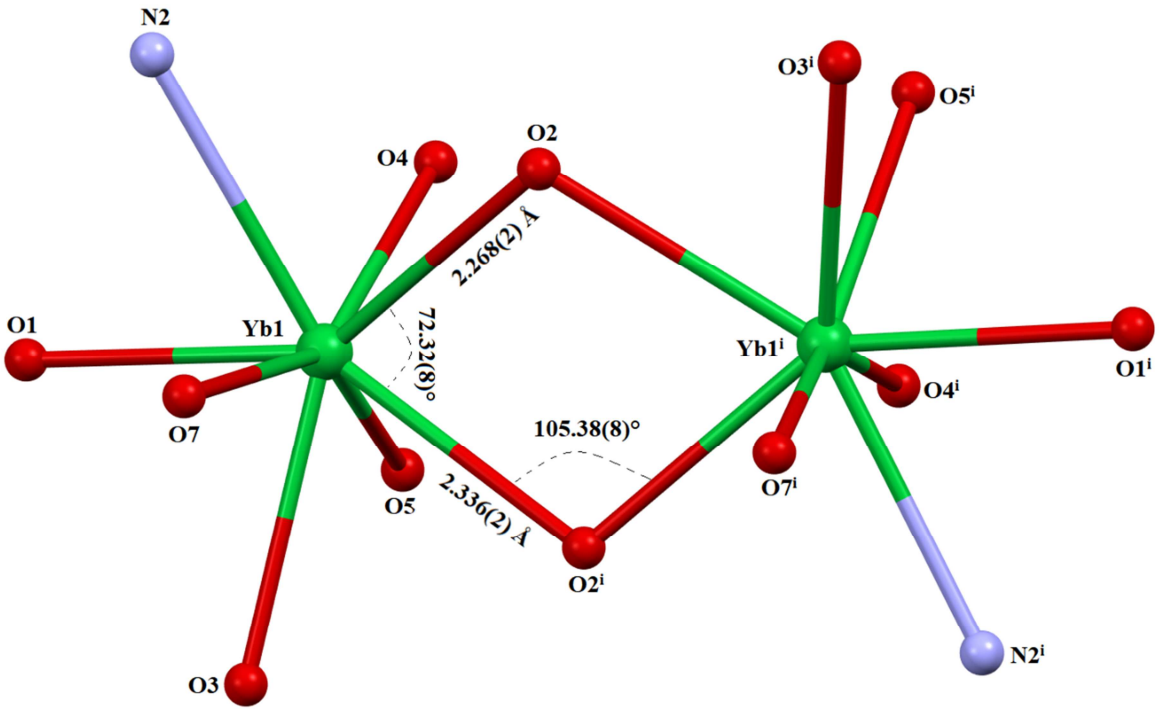

Figure 3. *Coordination polyhedron of the complex.*

Table 2. *Crystal data, X-ray data collection, data reduction and structure refinement for 3.*

Chemical formula	$C_{36}H_{40}Yb_2N_6O_{12}S_2$
Mr	1158.96
Crystal system, space group	Monoclinic, C2/c
Temperature (K)	173
a (Å)	13.0391 (6)
b (Å)	15.1199 (6)
c (Å)	20.7239 (7)
β (°)	105.671 (2)
V (Å^3)	3933.8 (3)
Z	4
Radiation type	Mo Kα
μ (mm^{-1})	4.91
Crystal size (mm)	0.10 × 0.09 × 0.09
No. of measured, independent and observed [I > 2σ(I)] reflections	55600, 5551, 4664
Rint	0.041
R[F^2 > 2σ(F^2)], wR(F^2), S	0.025, 0.065, 1.05
No. of reflections	5551
No. of parameters	265
Δρmax, Δρmin (e Å^{-3})	1.78, −0.70

Table 3. *Selected geometric parameters (Å, °).*

Yb1—O1	2.221 (3)	Yb1—O4	2.347 (2)
Yb1—O2	2.268 (2)	Yb1—O5	2.376 (2)
Yb1—O7	2.293 (2)	Yb1—O3^i	2.383 (2)
Yb1—O2^i	2.336 (2)	Yb1—N2	2.414 (3)
O1—Yb1—O2	143.90 (8)	O7—Yb1—O5	149.82 (8)
O2—Yb1—O2^i	72.32 (8)	O2^i—Yb1—O5	80.87 (8)
O7—Yb1—O4	153.47 (8)	O1—Yb1—N2	66.96 (9)
O2^i—Yb1—O4	105.02 (8)	O2—Yb1—N2	77.01 (9)
O2—Yb1—O5	120.08 (9)	Yb1—O2—Yb1^i	105.38 (8)

Symmetry code: (i) −x+1, y, −z+3/2.

The Yb1—O2—Yb1^i and O2—Yb1—O2^i angles of 105.38 (8)° and 72.32 (8)°, respectively, are in accordance with the value reported for the complex $Yb_2(L)_2(NO_3)_2{\cdot}2H_2O$ where H_2L is bis(N-salicylidene)-3-oxapentane-1,5-diamine [40]. The ytterbium—phenolate oxygen atom distances Yb1—O and Yb1—O2^i of 2.268 (2) Å and 2.336 (2) Å, respectively, agree with those for the phenolate oxygen atom in a bridging position [40, 41]. The Yb1—Yb1^i distance of 3.6615 (2) Å is comparable with the value of 3.607 (4) Å found for the complex $[Yb_2(\mu\text{-}\{(Me_2ArO)_2Me_2\text{-cyclam}\})I_2(thf)_2$ in which $H_2(Me_2ArO)_2Me_2$-cyclam is 1,4,8,11-tetraazacyclotetradecane-based bis(phenol) [42]. In the complex the Yb—N bond involving the azomethine nitrogen atom show the largest metal-distances [2.414 (2) Å] as found in the literature [43]. The Yb—O bonds involving the hydrazonic oxygen atoms is Yb1—O1 distance [2.221 (2) Å] is shorter than that of the Yb1—O7 bonds involving the dimethyl sulfoxide oxygen atoms [2.293 (2) Å]. The Yb1—O3 bond involving the methoxy oxygen atom [2.383 (3) Å] is the largest Yb—O bonds distances. The Yb—$O_{acetate}$ distances are 2.347 (2) Å and 2.376 (2) Å and are in the range expected for η^2-$OOCH_3$ [44]. The aromatic rings C1/C2/C3/C4/N3/C6 and C9/C10/C11/C12/C13/C14 of the ligand molecule are twisted with dihedral angle of 29.23 (1)° between their mean planes. The five membered ring Yb1O1C7N1N2 and the six membered ring Yb1O2C10C9C8N2 formed by the ligand, upon coordination to the Yb^{III}, are not coplanar. Their mean planes form a dihedral angle of 9.086 (3)°. The environment around the Yb ion is best described as a square antiprismatic. The coordination polyhedron of the complex 3 is illustrated in Figure 3.

4. Conclusion

The present work describes the results of the preparation of lanthanides complexes using the organic ligand *N*'-(2-hydroxy-3-methoxybenzylidene)nicotinohydrazide. The lanthanides (Y, Ce, Yb, Sm, Pr, Gd, and Tb) complexes formed are stable in air and in DMF solution. According to the data of elemental analysis, molar conductivity, FT-IR and UV–Vis spectra, and X-ray crystallographic structure determination, these complexes are neutral in nature and have a metal to hydrazone stoichiometry of 1:1. The acetate anions act in η^2-mode, while the dideprotonated ligand acts in μ_2-mode. All the observations reported in this paper are indicative of the coordination of the ligand in its iminol form. In all complexes the lanthanide ions are eight-coordinated, and the coordination geometry cans be described as a square antiprismatic.

Supplementary Material

CCDC-2251115 contains the supplementary crystallographic data for this paper. These data can be obtained free of charge via https://www.ccdc.cam.ac.uk/structures/, or by emailingdata_request@ccdc.cam.ac.uk, or by contacting The Cambridge Crystallographic Data Centre, 12 Union Road, Cambridge CB2 1EZ, UK.

References

[1] Anastasiadis, N. C., Mylonas-Margaritis, I., Psycharis, V., Raptopoulou, C. P., Kalofolias, D. A., Milios, C. J., Klouras, N. & Perlepes, S. P. (2015). Dinuclear, tetrakis (acetato)-bridged lanthanide (III) complexes from the use of 2-acetylpyridine hydrazone. Inorganic Chemistry Communications, 51, 99–102. https://doi.org/10.1016/j.inoche.2014.11.004

[2] Madanhire, T., Davids, H., Pereira, M. C., Hosten, E. C. & Abrahams, A. (2020). Synthesis, characterisation and anticancer activity screening of lanthanide (III) acetate complexes with benzohydrazone and nicotinohydrazone ligands. Polyhedron, 184, 114560. https://doi.org/10.1016/j.poly.2020.114560

[3] Soliman, S. M. & El-Faham, A. (2018). Low temperature X-ray structure analyses combined with NBO studies of a new heteroleptic octa-coordinated Holmium (III) complex with N,N,N-tridentate hydrazono-phthalazine-type ligand. Journal of Molecular Structure, 1157, 222–229. https://doi.org/10.1016/j.molstruc.2017.12.016

[4] Li, H.-G., Yang, Z.-Y., Wang, B.-D. & Wu, J.-C. (2010). Synthesis, crystal structure, antioxidation and DNA-binding properties of the Ln complexes with 1-phenyl-3-methyl-5-hydroxypyrazole-4-carbaldhyde-(benzoyl)hydrazone. Journal of Organometallic Chemistry, 695 (3), 415–422. https://doi.org/10.1016/j.jorganchem.2009.10.032

[5] Biswas, S., Das, S., Rogez, G. & Chandrasekhar, V. (2016). Hydrazone-Ligand-Based Homodinuclear Lanthanide Complexes: Synthesis, Structure, and Magnetism. European Journal of Inorganic Chemistry, 2016 (20), 3322–3329. https://doi.org/10.1002/ejic.201600335

[6] Kaczmarek, M. T., Zabiszak, M., Nowak, M. & Jastrzab, R. (2018). Lanthanides: Schiff base complexes, applications in cancer diagnosis, therapy, and antibacterial activity. Coordination Chemistry Reviews, 370, 42–54. https://doi.org/10.1016/j.ccr.2018.05.012

[7] Crutchley, R. J. (2014). Applications of lanthanide compounds to materials science and biology. Coordination Chemistry Reviews, 273–274, 1. https://doi.org/10.1016/j.ccr.2014.04.011

[8] Singh, K., Srivastava, P. & Patra, A. K. (2016). Binding interactions with biological targets and DNA photocleavage activity of Pr (III) and Nd (III) complexes of dipyridoquinoxaline. Inorganica Chimica Acta, 451, 73–81. https://doi.org/10.1016/j.ica.2016.07.003

[9] Das Mukherjee, D., Kumar, N. M., Tantak, M. P., Das, A., Ganguli, A., Datta, S., Kumar, D. & Chakrabarti, G. (2016). Development of Novel Bis(indolyl)-hydrazide–Hydrazone Derivatives as Potent Microtubule-Targeting Cytotoxic Agents against A549 Lung Cancer Cells. Biochemistry, 55 (21), 3020–3035. https://doi.org/10.1021/acs.biochem.5b01127

[10] Zabiszak, M., Nowak, M., Gabryel, M., Ogawa, K., Kaczmarek, M. T., Hnatejko, Z. & Jastrzab, R. (2019). New Coordination compounds of citric acid and polyamines with lanthanides ions – potential application in monitoring the treatment of cancer diseases. Biochemistry, 198, 110715. https://doi.org/10.1016/j.jinorgbio.2019.110715

[11] Ashma, A., Yahya, S., Subramani, A., Tamilarasan, R., Sasikumar, G., Ali, S. J. A., Al-Lohedan, H. A. & Karnan, M. (2022). Synthesis of new nicotinic acid hydrazide metal complexes: Potential anti-cancer drug, supramolecular architecture, antibacterial studies and catalytic properties. Journal of Molecular Structure, 1250, 131860. https://doi.org/10.1016/j.molstruc.2021.131860

[12] Aruna, V. A. J. & Alexander, V. (1996). Synthesis of lanthanide (III) complexes of a 20-membered hexaaza macrocycle. J. Chem. Soc., Dalton Trans., (9), 1867–1873. https://doi.org/10.1039/DT9960001867

[13] Ge, Y., Huang, Y., Wang, G., Li, Y. & Yao, J. (2020). A series of mononuclear lanthanide complexes constructed by Schiff base and β-diketonate ligands: synthesis, structures, magnetic and fluorescent properties. Polyhedron, 187, 114651. https://doi.org/10.1016/j.poly.2020.114651

[14] Yang, H., Liu, S.-S., Meng, Y.-S., Zhang, Y.-Q., Pu, L. & Yu, X.-Q. (2019). Magnetic properties and theoretical calculations of mononuclear lanthanide complexes with a Schiff base coordinated to Ln (III) ion in a monodentate coordination mode. Inorganica Chimica Acta, 494, 8–12. https://doi.org/10.1016/j.ica.2019.04.051

[15] Ndiaye-Gueye, M., Dieng, M., Thiam, E. I., Lo, D., Barry, A. H., Gye, M. & Retailleau, P. (2017). Lanthanide (III) Complexes with Tridentate Schiff Base Ligand, Antioxidant Activity and X-Ray Crystal Structures of the Nd (III) and Sm (III) Complexes. South African Journal of Chemistry, 70, 8–15. http://dx.doi.org/10.17159/0379-4350/2017/v70a2

[16] Lekha, L., Raja, K. K., Rajagopal, G. & Easwaramoorthy, D. (2014). Schiff base complexes of rare earth metal ions: Synthesis, characterization and catalytic activity for the oxidation of aniline and substituted anilines. Journal of Organometallic Chemistry, 753, 72–80. https://doi.org/10.1016/j.jorganchem.2013.12.014

[17] Yuan, B., Wang, F., Tao, J., Li, M. & Yang, X. (2019). Self-assembly of one visible and NIR luminescent Sm (III) coordination polymer with flexible Schiff base ligand. Inorganica Chimica Acta, 490, 24–28. https://doi.org/10.1016/j.ica.2019.02.019

[18] Yuan, B., Tao, J., Wang, F., Zhu, C., Li, M. & Yang, X. (2020). Construction of NIR luminescent nanoscale lanthanide complexes with new flexible Schiff base ligands. Journal of Rare Earths, 38 (2), 143–147. https://doi.org/10.1016/j.jre.2019.02.014

[19] Dang, S., Yu, J.-B., Wang, X.-F., Guo, Z.-Y., Sun, L.-N., Deng, R.-P., Feng, J., Fan, W.-Q. & Zhang, H.-J. (2010). A study on the NIR-luminescence emitted from ternary lanthanide [Er (III), Nd (III) and Yb (III)] complexes containing fluorinated-ligand and 4,5-diazafluoren-9-one. Journal of Photochemistry and Photobiology A: Chemistry, 214 (2), 152–160. https://doi.org/10.1016/j.jphotochem.2010.06.019

[20] Chandrasekhar, V., Bag, P., Speldrich, M., van Leusen, J. & Kögerler, P. (2013). Synthesis, Structure, and Magnetic Properties of a New Family of Tetra-nuclear {Mn2IIILn2}(Ln = Dy, Gd, Tb, Ho) Clusters With an Arch-Type Topology: Single-Molecule Magnetism Behavior in the Dysprosium and Terbium Analogues. Inorganic Chemistry, 52 (9), 5035–5044. https://doi.org/10.1021/ic302742u

[21] Shibasaki, M. & Yoshikawa, N. (2002). Lanthanide Complexes in Multifunctional Asymmetric Catalysis. Chemical Reviews, 102 (6), 2187–2210. https://doi.org/10.1021/cr010297z

[22] Kitamura, Y., Azuma, Y., Katsuda, Y. & Ihara, T. (2020). Catalytic formation of luminescent lanthanide complexes using an entropy-driven DNA circuit. Chem. Commun., 56 (27), 3863–3866. https://doi.org/10.1039/D0CC00602E

[23] Baykal, U. & Akkaya, E. U. (1998). Synthesis and phosphodiester transesterification activity of the La^{3+}-complex of a novel functionalized octadentate ligand. Tetrahedron Letters, 39 (32), 5861–5864. https://doi.org/10.1016/S0040-4039(98)01166-6

[24] Zeng, R., Sheng, H., Zhang, Y., Feng, Y., Chen, Z., Wang, J., Chen, M., Zhu, M. & Guo, Q. (2014). Heterobimetallic Dinuclear Lanthanide Alkoxide Complexes as Acid–Base Difunctional Catalysts for Transesterification. The Journal of Organic Chemistry, 79 (19), 9246–9252. https://doi.org/10.1021/jo5016536

[25] Vaughn, B. A., Koller, A. J., Chen, Z., Ahn, S. H., Loveless, C. S., Cingoranelli, S. J., Yang, Y., Cirri, A., Johnson, C. J., Lapi, S. E., Chapman, K. W. & Boros, E. (2021). Homologous Structural, Chemical, and Biological Behavior of Sc and Lu Complexes of the Picaga Bifunctional Chelator: Toward Development of Matched Theranostic Pairs for Radiopharmaceutical Applications. Bioconjugate Chemistry, 32 (7), 1232–1241. https://doi.org/10.1021/acs.bioconjchem.0c00574

[26] Woods, M., Kovacs, Z. & Sherry, A. D. (2002). Targeted Complexes of Lanthanide (III) Ions as Therapeutic and Diagnostic Pharmaceuticals. Journal of Supramolecular Chemistry, 2 (1), 1–15. https://doi.org/10.1016/S1472-7862(02)00072-2

[27] Bhiri, N. M., Dammak, M., Carvajal, J. J., Aguiló, M., Díaz, F. & Pujol, M. C. (2022). Stoichiometric dependence and laser heating effect on the luminescence thermometric performance of Er^{3+}, Yb^{3+}: $YuGdwVO_4$ microparticles in the non-saturation regime. Materials Research Bulletin, 151, 111801. https://doi.org/10.1016/j.materresbull.2022.111801

[28] Tamboura, F. B., Haba, P. M., Gaye, M., Sall, A. S., Barry, A. H. & Jouini, T. (2004). Structural studies of bis-(2,6-diacetylpyridine-bis-(phenylhydrazone)) and X-ray structure of its Y (III), Pr (III), Sm (III) and Er (III) complex. Polyhedron, 23 (7), 1191–1197. https://doi.org/10.1016/j.poly.2004.01.014

[29] Tamboura, F. B., Diop, M., Gaye, M., Sall, A. S., Barry, A. H. & Jouini, T. (2003). X-ray structure and spectroscopic properties of some lanthanides (III) complexes derived from 2,6-diacetylpyridine-bis(benzoylhydrazone). Inorganic Chemistry Communications, 6 (8), 1004–1010. https://doi.org/10.1016/S1387-7003(03)00167-9

[30] Tamboura, F. B., Diouf, O., Barry, A. H., Gaye, M. & Sall, A. S. (2012). Dinuclear lanthanide (III) complexes with large-bite Schiff bases derived from 2,6-diformyl-4-chlorophenol and hydrazides: Synthesis, structural characterization, and spectroscopic studies. Polyhedron, 43 (1), 97–103. https://doi.org/10.1016/j.poly.2012.06.025

[31] Sheldrick, G. M. (2015). SHELXT – Integrated space-group and crystal-structure determination. Acta Crystallographica Section A, 71 (1), 3–8. https://doi.org/10.1107/S2053273314026370

[32] Sheldrick, G. M. (2015). Crystal structure refinement with SHELXL. Acta Crystallographica Section C, 71 (1), 3–8. https://doi.org/10.1107/S2053229614024218

[33] Farrugia, L. J. (2012). WinGX and ORTEP for Windows: an update. Journal of Applied Crystallography, 45 (4), 849–854. https://doi.org/10.1107/S0021889812029111

[34] Haba, P. M., Tamboura, F. B., Diouf, O., Gaye, M., Sall, A. S., Baldé, C. A. & Slebodnick, C. (2016). Preparation, spectroscopic studies and x-ray structure of homobinuclear lanthanide (III) complexes derived from 2,6-diformyl-4-chlorophénol-bis-(2'-hydroxy-benzoylhydrazone). Bulletin of the Chemical Society of Ethiopia, 20 (1), 45–54. https://doi.org/10.4314/bcse.v20i1.21142

[35] Bakale, R. P., Naik, G. N., Machakanur, S. S., Mangannavar, C. V., Muchchandi, I. S. & Gudasi, K. B. (2018). Structural characterization and antimicrobial activities of transition metal complexes of a hydrazone ligand. Journal of Molecular Structure, 1154, 92–99. https://doi.org/10.1016/j.molstruc.2017.10.035

[36] Singh, Y. P., Patel, R. N., Singh, Y., Butcher, R. J., Vishakarma, P. K. & Singh, R. K. B. (2017). Structure and antioxidant superoxide dismutase activity of copper (II) hydrazone complexes. Polyhedron, 122, 1–15. https://doi.org/10.1016/j.poly.2016.11.013

[37] Salah, B. A., Kandil, A. T. & El-Nasser, M. G. A. (2019). Synthesis, molecular docking, and computational studies of novel hydrazone complexes. Journal of Radiation Research and Applied Sciences, 12 (1), 413–422. https://doi.org/10.1080/16878507.2019.1683273

[38] Geary, W. J. (1971). The use of conductivity measurements in organic solvents for the characterization of coordination compounds. Coordination Chemistry Reviews, 7 (1), 81–122. https://doi.org/10.1016/S0010-8545(00)80009-0

[39] Van Vleck, J. H. & Frank, A. (1929). The Effect of Second Order Zeeman Terms on Magnetic Susceptibilities in the Rare Earth and Iron Groups. Physical Review, 34 (11), 1494–1496. https://doi.org/10.1103/PhysRev.34.1494

[40] Wu, H., Pan, G., Bai, Y., Wang, H., Kong, J., Shi, F., Zhang, Y. & Wang, X. (2015). Synthesis, structure, antioxidation, and DNA-binding studies of a binuclear ytterbium (III) complex with bis(N-salicylidene)-3-oxapentane-1,5-diamine. Research on Chemical Intermediates, 41 (6), 3375–3388. https://doi.org/10.1007/s11164-013-1440-5

[41] Chen, W.-B., Zhong, L., Zhong, Y.-J., Zhang, Y.-Q., Gao, S. & Dong, W. (2020). Understanding the near-infrared fluorescence and field-induced single-molecule-magnetic properties of dinuclear and one-dimensional-chain ytterbium complexes based on 2-hydroxy-3-methoxybenzoic acid. Inorganic Chemistry Frontiers, 7 (17), 3136–3145. https://doi.org/10.1039/D0QI00628A

[42] Maria, L., Sousa, V. R., Santos, I. C., Mora, E. & Marçalo, J. (2016). Synthesis and structural characterization of polynuclear divalent ytterbium complexes supported by a bis(phenolate) cyclam ligand. Polyhedron, 119, 277–285. https://doi.org/10.1016/j.poly.2016.09.008

[43] Anwar, M. U., Dawe, L. N., Tandon, S. S., Bunge, S. D. & Thompson, L. K. (2013). Polynuclear lanthanide (Ln) complexes of a tri-functional hydrazone ligand – mononuclear (Dy), dinuclear (Yb, Tm), tetranuclear (Gd), and hexanuclear (Gd, Dy, Tb) examples. Dalton Trans., 42 (21), 7781–7794. https://doi.org/10.1039/C3DT32732A

[44] He, H., Sykes, A. G., May, P. S. & He, G. (2009). Structure and photophysics of near-infrared emissive ytterbium (III) monoporphyrinate acetate complexes having neutral bidentate ligands. Dalton Trans., (36), 7454–7461. https://doi.org/10.1039/B909243A